Streamer Velocity at the Breakdown of an Air Gap with a Sharply Inhomogeneous Distribution of Electric Field Strength

D.A. Sorokin
SDmA-70@loi.hcei.tsc.ru

V.F. Tarasenko, G.V. Naidis, D.V. Beloplotov, M.I. Lomaev, N.Yu. Babaeva

Institute of High Current Electronics SB RAS, 634055, Russia Tomsk, 2/3 Akademicheskii Ave.
Joint Institute for High Temperatures RAS, 125412, Russia, Moscow, Izhorskaya Str. 13 Bd.2

Introduction

In recent years, there has been a high interest in the study of the

High-voltage nanosecond discharge in gaps with strongly inhomogeneous electric field strength distribution filled with dense gases, including atmospheric-pressure air [1]

Conditions for implementation:

1) at least one of the electrodes must have a small radius of curvature (tube, cone, needle, blade);

2) high-voltage pulse: tens-hundreds kV; short rise time: fractions-ones ns.

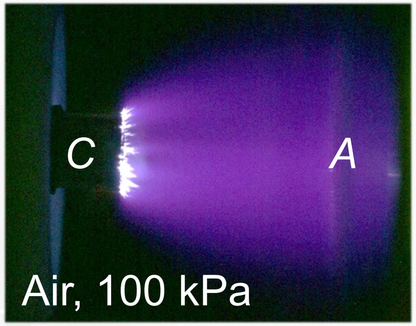

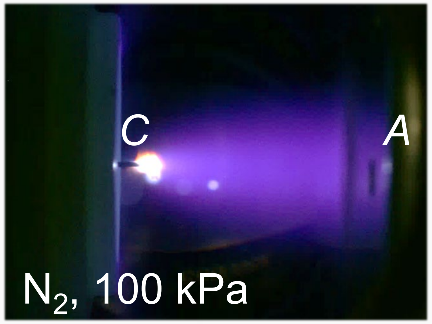

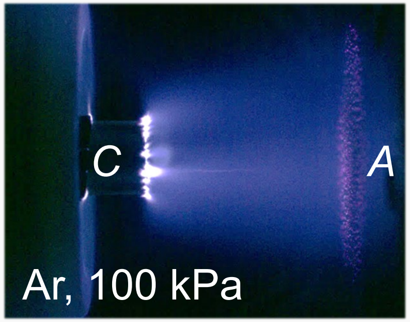

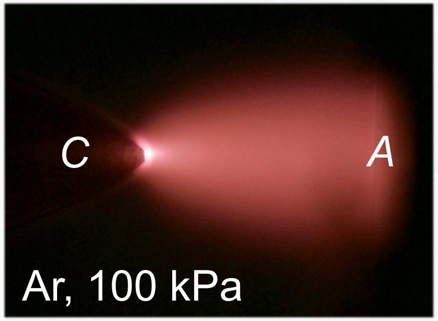

Features:

1. Diffuse form of discharge combustion at high-pressures of atomic and molecular gases and in their mixtures, i.e. generation of dense non-equilibrium low-temperature plasma (reactive cold plasma).
2. Generation of high-energy electron flows (including runaway electrons) and X-ray [2].
3. High input power density: up to 1 GW·cm^{-3}.

[1]. Runaway Electrons Preionized Diffuse Discharges // Edited by V. F. Tarasenko. – Nova Science Publishers, Inc., NY, USA, 2014.
[2]. Generation of Runaway Electron Beams and X-Rays in High Pressure Gases. Edited by V.F. Tarasenko. Nova Science Publishers, Inc., NY, USA, 2016.

Introduction

Diffuse discharges are widely used for scientific purposes and have great potential for use as a basis for technical devices and technological processes [3-5].

Despite the fact that this type of discharge was discovered half a century ago [6], there are still many questions related to the mechanisms of its ignition and combustion. The processes leading to the ignition of a diffuse discharge occur at extremely small spatial and temporal scales, which requires the use of experimental techniques with high resolution, both spatial and temporal. It should be said that the latest advances in technology make it possible to study processes with femtosecond (and, possibly, shorter) temporal resolution at nanoscales (and even less) and obtain reliable results. This circumstance, as well as progress in the development of the theory and numerical modeling of this phenomenon, have made it possible in recent years to obtain a number of the most important results that partially answer the above questions. For example, it was found that the breakdown of the «point (needle)-plane" gap occurs in the form of a streamer, the transverse dimensions of which can reach the length of the interelectrode gap (up to 8 cm) [7, 8]. However, there are very few works where the streamers' velocities in the gap obtained experimentally and computationally are compared.

Main objective: experimental and theoretical study of the streamer speed, which ensures the breakdown of the gap during the ignition of a high-voltage nanosecond discharge in air at atmospheric pressure under conditions of a highly inhomogeneous distribution of the electric field strength.

[3]. R. Hippler, H. Kersten, M. Schmidt, and K.H. Schoenbach (eds), Low Temperature Plasma: Fundamentals, Technologies, and Techniques (WILEY-VCH Verlag, 2008).
[4]. P. K. Chu and X. Lu (eds), Low Temperature Plasma Technology (CRC Press, 2014).
[5]. I. Adamovich et al. The Plasma Roadmap. Low temperature plasma science and technology. J.Phys.D.Appl.Phys. ***50*** *323001 (2017).*
[6]. L.V. Tarasova, L.N. Khudyakova, Sov. Phys. Tech. Phys. ***14*** *1148 (1969).*
[7]. D.V. Beloplotov et al.. Streamers at the subnanosecond breakdown of argon and nitrogen in nonuniform electric field at both polarities // Tech. Phys. 63 793 (2018).
[8]. V.F. Tarasenko, G.V. Naidis, D.V. Beloplotov, I.D. Kostyrya, and N.Yu. Babaeva, Plasma Phys. Rep. ***44*** *746 (2018).*

Experimental Setup

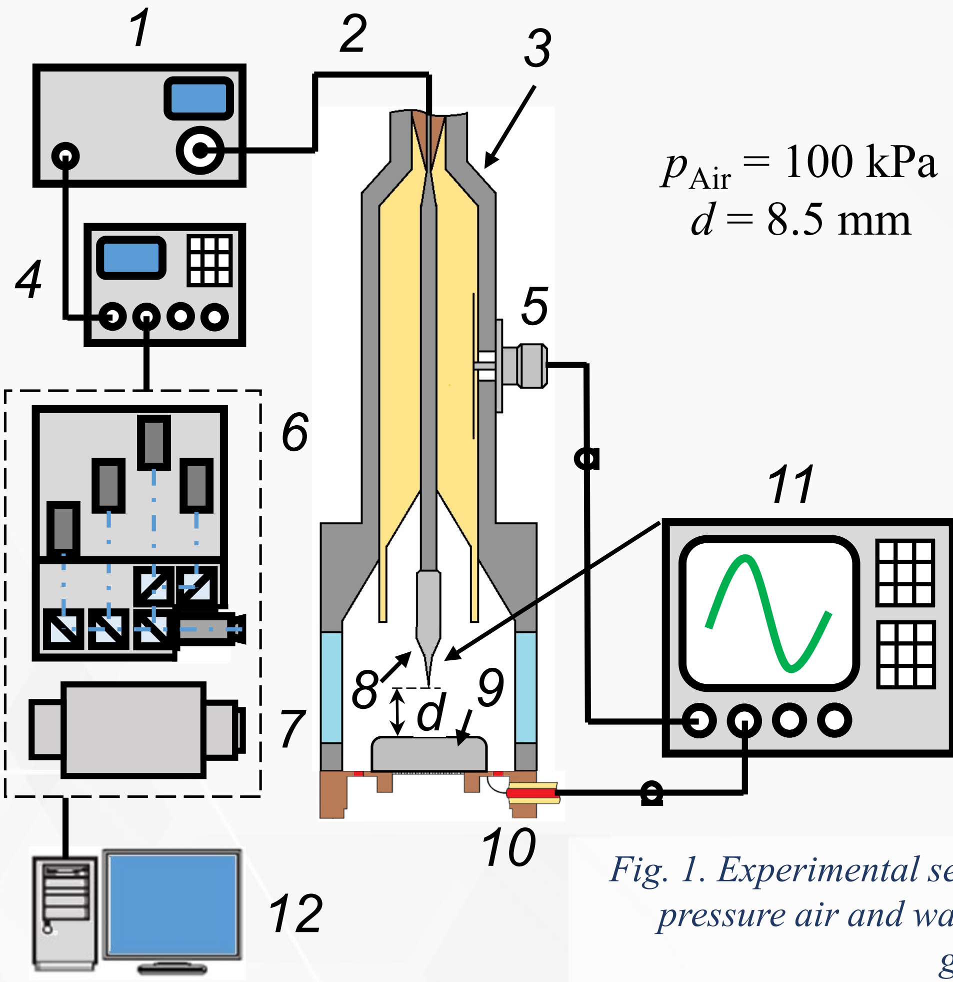

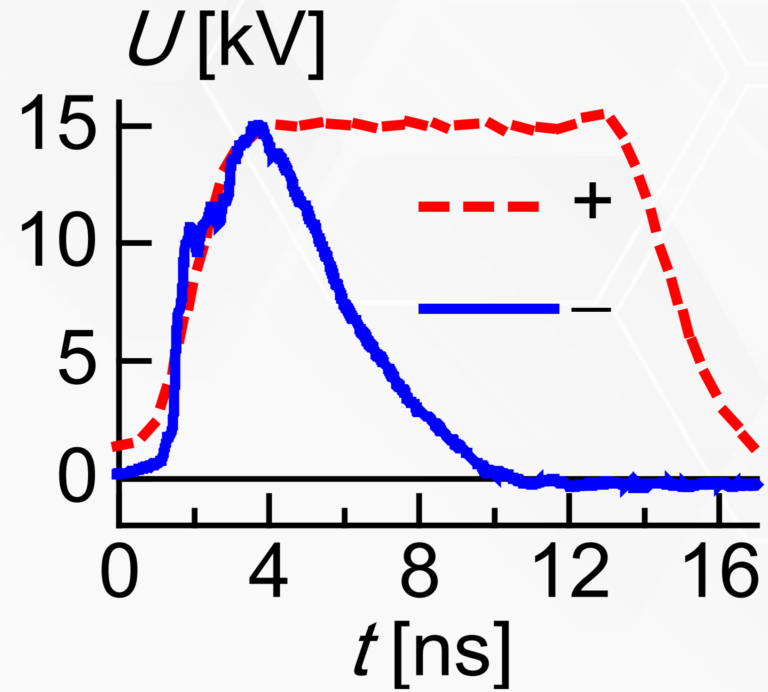

Fig. 1. Experimental setup for studying development of discharge in atmospheric-pressure air and waveforms of voltage pulses (incident waves) produced by generators GIN-50-1 and GIN-100-1.

1 – HV generators: GIN-50-1 (U_0 = +15 kV; $\tau_{0.2\text{-}0.9}$ = 2.2 ns; $\tau_{0.5}$ = 13 ns) and GIN-100-1 (U_0 = +15 kV; $\tau_{0.1\text{-}0.7}$ = 0.7 ns; $\tau_{0.5}$ = 4 ns); 2 – HV cable; 3 – transmission line (75 Ω); 4 – triggering generator BNC-565; 5 – capacitive voltage divider; 6 – ICCD camera HSFC Pro or streak-camera Hamamatsu C-10910-05 (200-900 nm); 7 – quartz windows; 8 – HV electrode (sewing needle); 9 – flat grounded electrode; 10 – current shunt made of chip-resistors; 11 – oscilloscope Tektronix 3054B (500 MHz; 5 GS/s); 12 – PC.

Results. Negative polarity

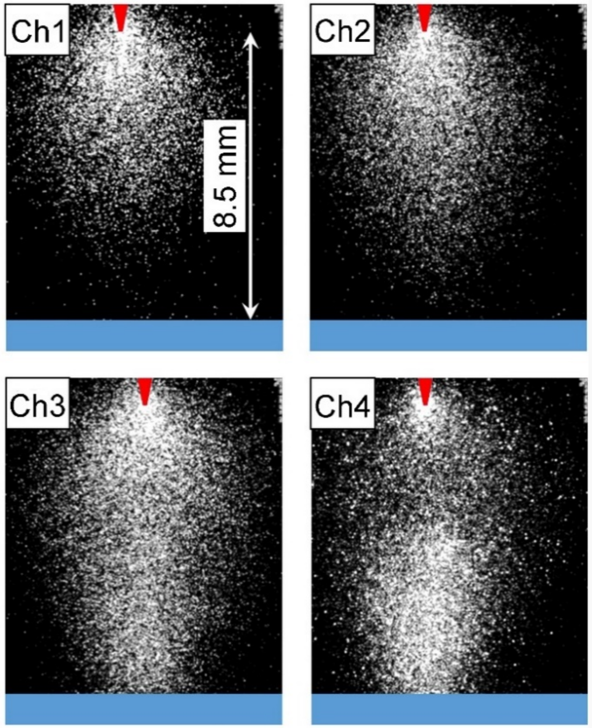

Fig. 2a. Plasma glow at different time instances. Ch1–Ch4 – are channels of ICCD camera.

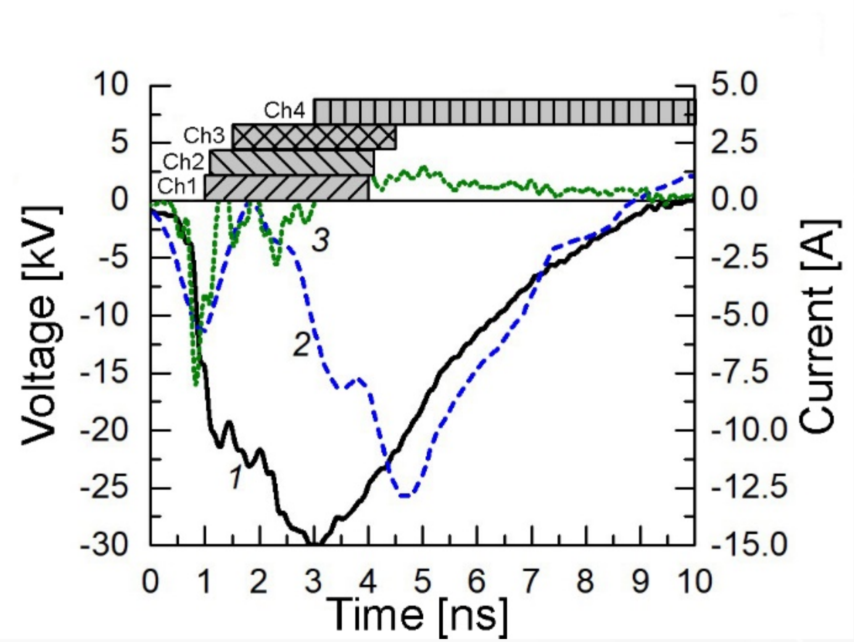

Fig. 2b. Waveforms of voltage (1), discharge current (2), and displacement current C×(dU/dt) (C – gap capacitance; U – gap voltage) (3). The rectangles denote the time of launching the ICCD camera channels. The length of rectangles corresponds to the duration of exposition.

A streamer is formed near a HV electrode with a small radius of curvature. At the initial stage, it has the shape of a "ball". Then, the streamer front is elongated along the longitudinal axis. and eventually bridges the interelectrode gap, leading to the ignition of a diffuse discharge in it.

The appearance and development of a streamer leads to a redistribution of the electric field strength in the gap and to the flow of a dynamic displacement current (DDC). The DDC magnitude is determined by the speed of the streamer along the gap and the change in its dimensions.

Results. Positive polarity

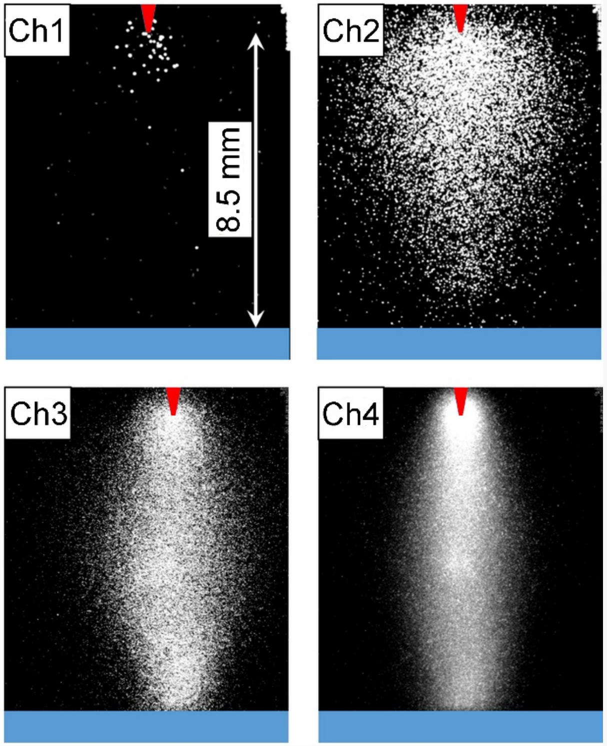

Fig. 3a. Plasma glow at different time instances. Ch1–Ch4 – are channels of ICCD camera.

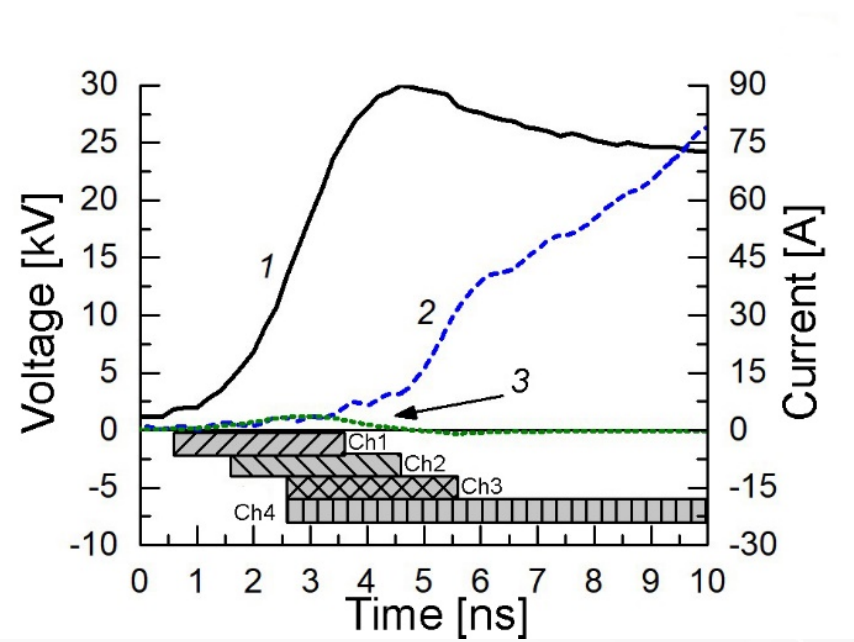

Fig. 3b. Waveforms of voltage (1), discharge current (2), and displacement current C×(dU/dt) (C – gap capacitance; U – gap voltage) (3). The rectangles denote the time of launching the ICCD camera channels. The length of rectangles corresponds to the duration of exposition.

With a positive polarity of the voltage pulse, the breakdown process does not qualitatively differ – a streamer with large transverse dimensions is also formed and propagates along the gap. With both polarities, the streamer appears at the same amplitude value of the voltage across the gap. Differences in the magnitude of the conduction current at different polarities, flowing after closing the gap with a streamer, are due to different duration of voltage pulses. At the stage of formation of positive and negative streamers, DDC reaches approximately the same values.

Results. Streamer speed. Experiment

$+U_0$ –

$-U_0$ –

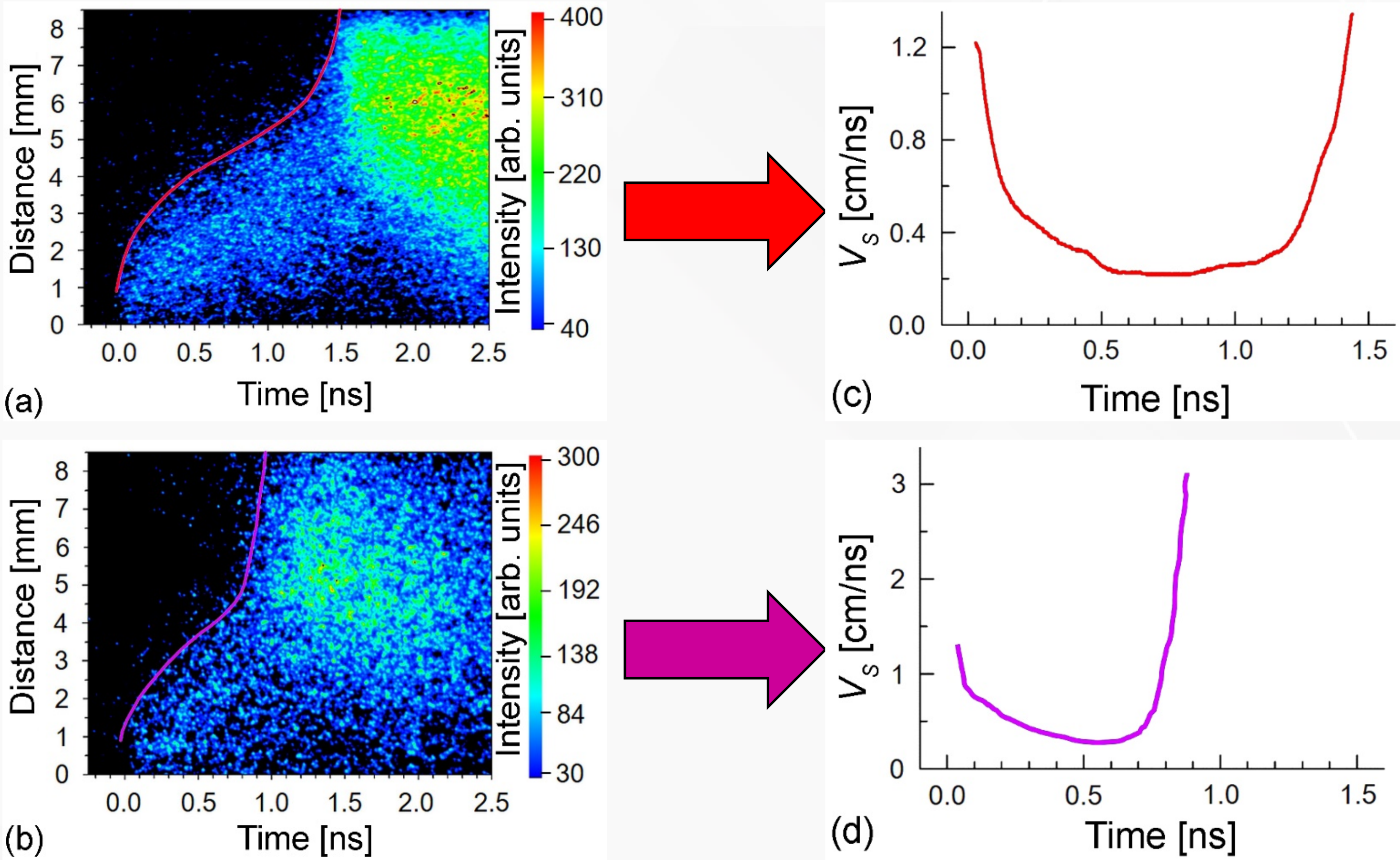

Fig. 4. Time behavior of plasma glow in the range 200-900 nm at the breakdown stage at positive (a) and negative (b) polarities and corresponding speed of the streamer front (c, d).

Under these conditions, the speed *Vs* (maximum and average) of a positive streamer is lower than that for a negative one. The streamer has the highest speed in the near-electrode zones. The streamer speed increases with increasing amplitude of the incident voltage wave. At high voltage, the breakdown of the air-filled gap occurs in a time of ~ 1 ns or less. With a negative polarity of an electrode with a small radius of curvature, runaway electrons are recorded behind a flat grounded anode, which provide ionization of the gas in the gap.

Results. Streamer speed. Modeling

Two-dimensional (axisymmetric) drift-diffusion model [9, 10] (includes the transport equations for the charged particles and the Poisson equation for the electric field; photoionization of a gas ahead the streamer front) was used in simulations.

initial concentrations of electrons and positive ions:
$n_e^0 = n_i^0 = 10^3\ cm^{-3}$
gap geometry: *"sphere–plane"*
radii of sphere electrode: $R_{sph} = 1$ *and* $1.5\ mm$
gap width: $d = 8.5$ mm
gas pressure: $p_{\mathrm{Air}} = 100$ kPa
incident voltage pulse amplitude: $U_0 = 20$ kV

The form of the dependence $V_s(t)$ obtained in the simulation coincides with the experimental one. However, the speed values are different. The average speed of the negative streamer obtained in the simulation turned out to be less than that of the positive one.

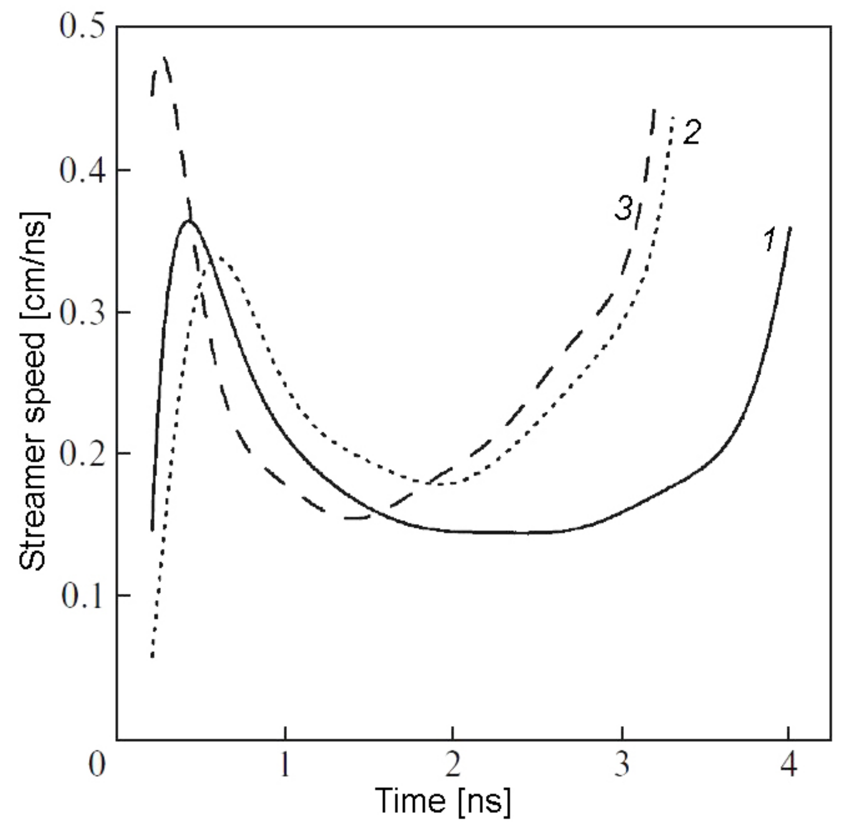

Fig. 5. Streamer speed at negative (1) and positive (2, 3) polarity of the voltage pulse. 1, 2 – R_{sph} = 1.5 mm; 3 – R_{sph} = 1 mm.

This may be due to the fact that, with a negative polarity of an electrode with a small radius of curvature, runaway electrons (RE) are generated in the gap, which effectively ionize the gas, thereby ensuring a faster propagation of the streamer.

Results. Streamer speed. Modeling

In order to take into account the effect of runaway electrons on the characteristics of the negative streamer, the following approach was used.
It is assumed that the RE quickly (before the start of the streamer) ionizing the gas create a thin channel with an increased concentration of charged particles, along which the negative streamer moves.

The concentration of electrons n_e^{ch} and positive ions n_i^{ch} along the channel is uniform.

The concentration of electrons and positive ions changes radially as:

$$n_e^r = n_i^r = n_{ch} \times [\exp(r/R_{ch})^2]$$

where r – distance from the channel axis; n_{ch} – particle concentration on the channel axis; R_{ch} – channel radius.

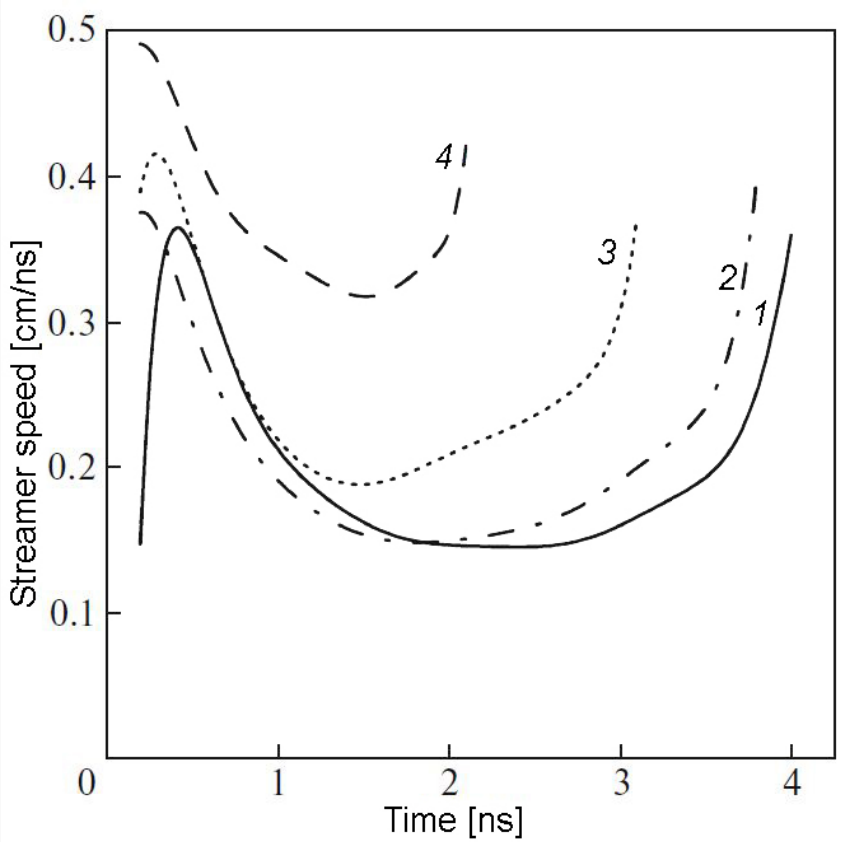

Fig. 6. Negative streamer speed vs. time: 1 – w/o channel; 2 – n_{ch} = 10^8 cm^{-3}, R_{ch} = 0.5 mm; 3 – n_{ch} = 10^8 cm^{-3}, R_{ch} = 0.2 mm; 4 – n_{ch} = 10^{10} cm^{-3}, R_{ch} = 0.2 mm. R_{sph} = 1.5 mm.

The approximation of constancy of the transverse size of the region with an increased level of preionization was used.
A channel with an increased initial concentration of charged particles significantly accelerates the streamer motion. The higher the concentration n_{ch} and the thinner the channel, the higher the average streamer speed. Thus, modes can be realized in which the average speed of a negative streamer is higher than that of a positive one (as in the experiment).

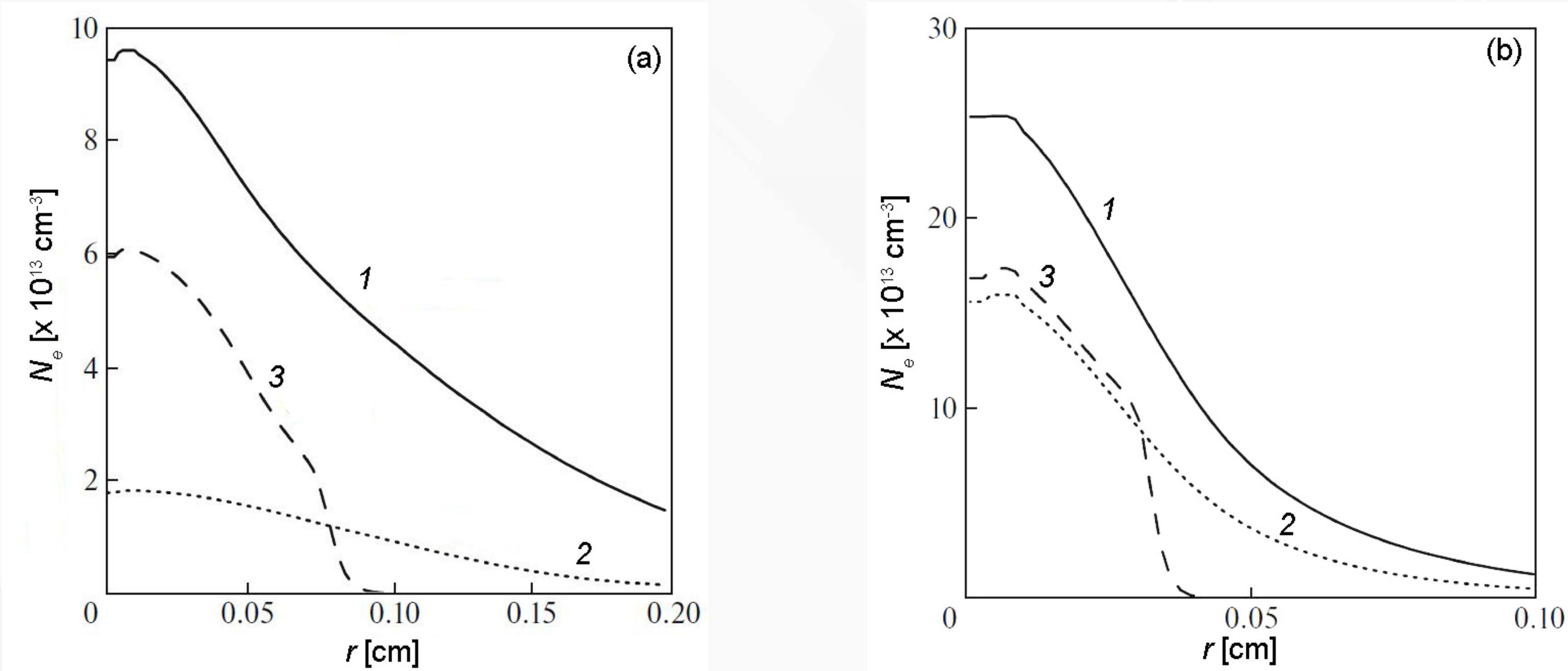

Fig. 7. Radial distributions of electron concentration at different distances z from cathode behind front of negative streamer. (a) – w/o channel; (b) – $n_{ch} = 10^{10}$ cm^{-3}, $R_{ch} = 0.2$ mm. 1 – 0.1 cm;, 2 – 0.4 cm; 3 – 0.7 cm. $R_{sph} = 1.5$ mm

Here, the width of the radial profile of $n_e(r)$ corresponds to the width of the streamer front in the given cross-section. In the absence of a channel (Fig. 7a), the half-width of the streamer near the cathode and in the middle of the gap is close to 1 mm and decreases approximately twofold as the front approaches the flat anode. In the presence of a channel (Fig. 7b),, the half-width of the streamer changes along the axis weakly, amounting to a value of about 0.3 mm, which is close to the channel radius. The presence of a narrow channel affects not only the streamer shape, but also the parameters of the streamer plasma: n_e on the axis is three times higher at the electrodes and almost an order of magnitude in the middle of the gap.

Results. Streamer speed. Modeling

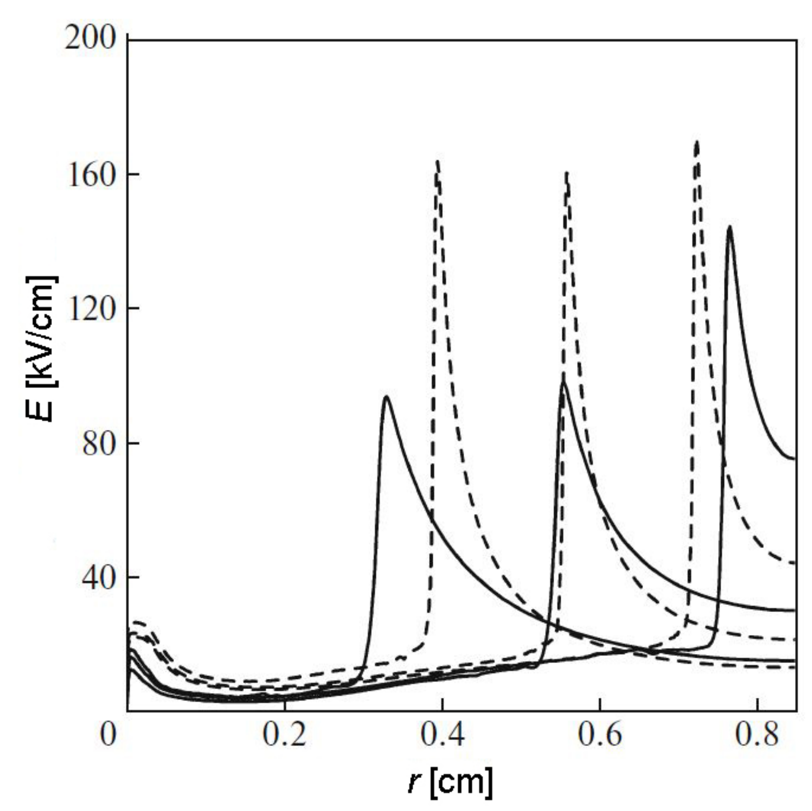

Fig. 8. Axial distributions of electric field strength at different time instances at propagation of negative streamers: the solid lines – w/o channel; the dashed lines – $n_{ch} = 10^{10}$ cm^{-3}, $R_{ch} = 0.2$ *mm .*

The channel with an increased concentration of charged particles also affects the profiles of the electric field during the movement of the streamer front: in the central part of the gap, the field in the streamer front increases approximately twofold. The streamer speed at its smaller radius is higher than in a homogeneous medium (without a channel), which is due to the higher value of the field in its front.

Conclusions

1. The experimental and simulation results indicate that when a nanosecond discharge is ignited in a “needle-plane” gap filled with atmospheric-pressure air under conditions of a strongly inhomogeneous electric field, the breakdown occurs in the form of a streamer with large transverse dimensions.
At the initial stage, a streamer with a shape close to spherical is formed near the high-voltage electrode with a small radius of curvature (pointed electrode). As the streamer moves away from the needle electrode and as the dimensions of the streamer tip increase, the streamer’s speed significantly decreases due to the decrease in the electric field in the gap. As the amplitude of the voltage pulse or/and as its duration decrease, the streamer can stop in the gap (streamer does not have time to form). The increase in the streamer’s speed near the planar electrode is caused by a repeated increase in the electric field. As the streamer approaches the planar electrode and under large amplitudes of the voltage pulse, its ball shape is preserved, and as the voltage decreases, the streamer’s diameter near the planar electrode decreases and the streamer takes the cylindrical shape. After the breakdown of the gap by the ball or cylindrical streamer, a diffuse discharge is formed in the gap. The duration of the diffuse discharge is limited by its transition to the spark stage, mostly due to the sparks’ leaders beginning from the electrode spots.

2. The speed of the streamer changes significantly as it moves along the gap. Under these conditions, the speed of the negative streamer is greater than the speed of the positive one. The highest streamer speeds are achieved when it starts from a high-voltage electrode with a small radius of curvature and when it approaches a flat grounded electrode.

3. It is shown that the generation of runaway electrons in the gap, in particular, with a negative polarity of the high-voltage tip electrode, significantly affects the streamer velocity, due to which the gap breaks down. Calculations have shown that photoionization alone ahead of the streamer front is not enough to explain the higher (as compared to the positive streamer) speeds of the negative streamer.

The work was supported by the Russian Foundation for Basic Research under grants Nos. 18-32-00103 and 17-52-16002.